

Extreme self-organization in networks constructed from gene expression data

Himanshu Agrawal

Department of Physics of Complex Systems, Weizmann Institute of Science, Rehovot 76100, Israel

(Dated: July 15, 2002)

We study properties of networks constructed from gene-expression data obtained from many types of carcinomas. The networks are constructed by connecting vertices that belong to each others list of K -nearest-neighbors, with K being an *a priori* selected non-negative integer. We introduce an order parameter for characterizing the homogeneity of the networks. On minimizing the order parameter with respect to K , degree distribution of the networks shows power-law behavior in the tails with an exponent of unity. Analysis of the eigenvalue spectrum of these networks confirms the presence of the power-law and small-world behavior. This shows that these gene networks contain a few very highly connected genes and a large number of genes with low connectivity. These results conclusively show that various carcinomas are a consequence of malfunction of a few genes that either regulate the expression of a large number of other genes or make the hubs of crowded regulatory pathways.

Recent technical advancements have lead to widespread use of gene chips for quantizing and monitoring the expression level of thousands of genes in parallel.^{1,2} Gene expression profiling has turned out to be an important tool for diagnosis and classification of diseases. It is being used extensively for identifying genes responsible for specific conditions, e.g., various types of carcinomas.^{3,4,5,6,7} This is done using specialized clustering techniques developed in recent years.^{8,9,10} Gene expression data can also be used for constructing networks of co-expressed and co-regulated genes. Since proteins are the end product of gene expression, various types of protein networks^{11,12} and gene networks are directly related. Consequently, networks of co-regulated genes are expected to play key role in biological processes. It is, thus, important to understand the properties of these networks. In this paper we outline results that show extremely high relevance of these networks in the functioning of biological organism.

The volume of gene expression data obtained from typical experiments is enormous and contains information on expression of all the genes (presently almost 10,000 or more) marked on the chip. In any given condition most of the genes are not important and do not express. As a result, before the expression data can be used for constructing networks, it requires extensive processing and filtering to eliminate uninformative genes. We skip these details here as they can be found with the source of the data^{3,4,5,6,7} and elsewhere.^{8,9} Henceforth, we assume that expression data for the selected set of informative genes is available in the form of a matrix having N rows and D columns. The columns represent the samples/tissues and rows represent the genes. Furthermore, the expression values of each of the genes in this matrix are normalized to have a mean of zero and variance of unity across the samples.

Method of construction of networks: The normalized expression levels of genes are treated as coordinates of N points (corresponding to the genes) in D dimensional space of samples. These points make the vertices of the networks. The network construction algorithm requires specification of the maximum number of neighbors K , $0 \leq K < N$, that a vertex can have. For a given K , the network is constructed using the following two step procedure. (i) For each vertex i , $i = 1, \dots, N$, make a list L_i of its first K nearest neighbors. (ii) Connect all vertices i and j through an edge if they belong to each others list of K nearest neighbors, i.e., vertices i and j are con-

nected if $i \in L_j$ and $j \in L_i$, otherwise the vertices i and j are not connected. This algorithm is derived from the K -nearest-neighbor parameter estimation method.¹³ With some heuristic modifications it has been used earlier in clustering analysis of various types of data.¹⁰ In our implementations, we used Euclidean norm as the distance measure for making the list of K nearest neighbors. Other distance measures can also be used. The results presented herein remain unaltered as long as the distance measure preserves the ordering of points obtained from the Euclidean measure.

For a given data set, the topological structure of networks generated by this algorithm depends strongly on the parameter K . For $K = 0$ the network consists of N isolated vertices and for $K = N - 1$ each vertex is connected to all the other vertices. For most of the values of K ($< N - 1$) these network have more than one connected component. As K increases, the connectivity of each vertex grows depending on its local environment. Vertices that lie close to each other tend to get mutually connected in preference to those lying farther away. Thus, all the connected components in these networks have a small-world structure. Furthermore, for $K \gtrsim 3$ a giant connected component is present in the networks.

Analysis of networks: We constructed and analyzed networks using several published gene expression data sets. To ensure that our results are not affected by possible bias of technology used for manufacturing the gene chips, we used expression data sets obtained using both oligonucleotide arrays^{3,4,5} as well as cDNA microarrays.^{6,7}

For each of the data sets, networks were constructed for all the possible values of K . For each network we calculated $P(z)$ the probability of finding a vertex of degree z . Since these networks are small, $P(z)$ is very noisy. As a result, we calculated the cumulative probability distribution function

$$F(z) = \sum_{i=z}^{z_{\max}} P(i) \quad (1)$$

where z_{\max} is the maximum degree in the network.

We also define a quantity $c = z + 1$. This quantity gives the size of the smallest cluster around a vertex with connectivity z that includes the vertex and its neighbors. It can also be considered as the size of a “droplet” that is formed by the vertex and its neighbors. Equivalently, it is the number of bonds attached to the vertex, z of which come from the neighbors and

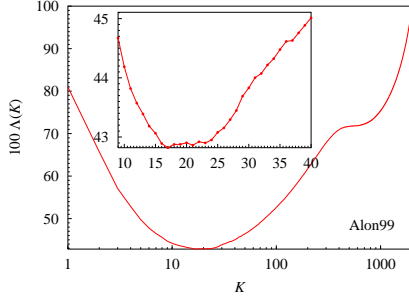


FIG. 1: Variation of $\Lambda(K)$ with K for networks constructed from the colon cancer data of Alon *et al.*³ The inset shows blow up of a small zone around the minima. The key “Alon99” corresponds to data set as described.³¹

1 comes from a “ghost” vertex which could be a source of externally applied field.¹⁴

Since, the smallest and the largest values of z are 0 and z_{\max} , the corresponding values for c become 1 and $c_{\max} = 1 + z_{\max}$, where c_{\max} is the largest droplet size. The probability density $\tilde{P}(c)$ and cumulative distribution $\tilde{F}(c)$ functions corresponding to c are defined similarly to those for z . The linear relationship of c and z implies that $\tilde{P}(c) = P(z)$ and $\tilde{F}(c) = F(z)$. Outside the range of z and c , the corresponding probability density functions are defined to be zero. Thus, $\tilde{F}(c)|_{c \leq 1} = F(z)|_{z \leq 0} = 1$, $\tilde{F}(c)|_{c > c_{\max}} = F(z)|_{z > z_{\max}} = 0$.

Order parameter: The homogeneity of the networks can be characterized by a single order parameter. We found that the area Λ enclosed by the $c^* = c/c_{\max}$ versus $\tilde{F}(c)$ curve (or equivalently $F(z)$ curve) between $c^* = 0$ and 1 is a suitable order parameter. It takes values in the range 0 to 1 depending on the homogeneity of the network. Since c_{\max} is finite and the values of c are evenly spaced, $\Lambda(K)$ is easily calculated using Simpson’s rule and is equal to

$$c_{\max} \Lambda(K) = \frac{1}{2} [1 - P(z_{\max})] + \sum_{i=0}^{z_{\max}} (i+1)P(i). \quad (2)$$

The terms with factor of 1/2 represent the area of strips at the boundary. The contribution of these terms vanishes as the number of strips increases. It is zero if $P(z)$ is a delta function.

From Eq. (2) the value of $c_{\max} \Lambda(K)$ is easily identified as the mean size $\bar{c} = 1 + \bar{z}$ of the droplets, where \bar{z} is the average degree of vertices in the network. Thus, $\Lambda(K)$ is the average droplet size normalized with the size of the largest droplet in the network. It is a measure of separation between the mean and maximum droplet sizes in the network. Thus, it also functions as an indicator of the overall behavior of $F(z)$ and $P(z)$. Very small values of $\Lambda(K)$ imply descending step like $F(z)$ with large tails corresponding to sharply peaked $P(z)$ with large tails. Values close to unity imply that $F(z)$ is flat and $P(z)$ has a small tail and is sharply peaked like a delta function. Intermediate values imply a decaying $F(z)$ with a spread out $P(z)$ having large heavy tails.

Fig. 1 shows the behavior of $\Lambda(K)$ for networks constructed using colon cancer data of Alon *et al.*³ The figure shows that as K is increased from 1 to $N - 1$, $\Lambda(K)$ initially decreases and

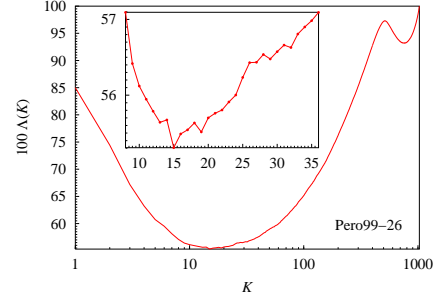


FIG. 2: Variation of $\Lambda(K)$ with K for networks constructed from breast cancer data of Perou *et al.*⁶ The inset shows blow up of a small zone around the minima. The key “Pero99-26” corresponds to data set as described.³¹

attains a minima at some value of $K = K_1$ (here $K_1 \approx 16$). The minima is nearly flat and persists till $K = K_2$ (here $K_2 \approx 24$). As K is increased beyond K_2 , $\Lambda(K)$ continues to increase and reaches its maximum value of 1 at $K = N - 1$.

It is also possible to obtain minima of $\Lambda(K)$ at other values of K between K_2 and $N - 1$, usually at $K \approx 3N/4$. This is usually a finite size affect. It can also happen if there is high inhomogeneity on length scales large compared to the nearest neighbors scale. These minima are very shallow compared to that between K_1 and K_2 because the probability density function corresponding to size of “droplets” on larger length scales are sharper compared to $P(z)$ and also have smaller tails. These higher order minima, however, are not relevant.

Behavior similar to that seen in Fig. 1 was observed in networks constructed from several other gene expression data sets also.^{4,5,6,7} Fig. 2 shows the behavior of $\Lambda(K)$ in networks constructed using breast cancer data of Perou *et al.*⁶ The figure shows a shallow second minima at $K \approx 3N/4$. This is a consequence of finite size. Figures for other data sets, being similar to Fig. 1 and 2, are omitted. A very shallow second minima was observed at $K \approx 3N/4$ in networks constructed using breast cancer data of Perou *et al.*⁷ also.

The behavior of $\Lambda(K)$ divides the networks in three classes.

- (i) The networks corresponding to $1 \leq K < K_1$ have few connections between vertices but they have high homogeneity.
- (ii) Those corresponding to $K_1 \leq K \leq K_2$ are somewhat better connected but are highly inhomogeneous.
- (iii) In the networks for $K_2 < K \leq N - 1$ the vertices have strong interconnections and high homogeneity that increases with K .

Cumulative probability distribution function: Fig. 3 shows the variation of the observed cumulative probability distribution function $F(z)$ with the normalized degree $(z+1)/(z_{\max}+1)$ in a wide range of values of K for networks constructed from several different gene expression data sets.^{3,4,5,6,7} In each of the graphs, the curves corresponding to different types of networks are drawn using different line styles. In the figure the curves corresponding to the range $1 \leq K < K_1$ (dashed lines) approach the solid circles as K increases. The curves corresponding to the range $K_2 < K \leq N - 1$ (dotted lines) go away from the solid circles as K is increased.

The most interesting behavior seen in Fig. 3 is that of the

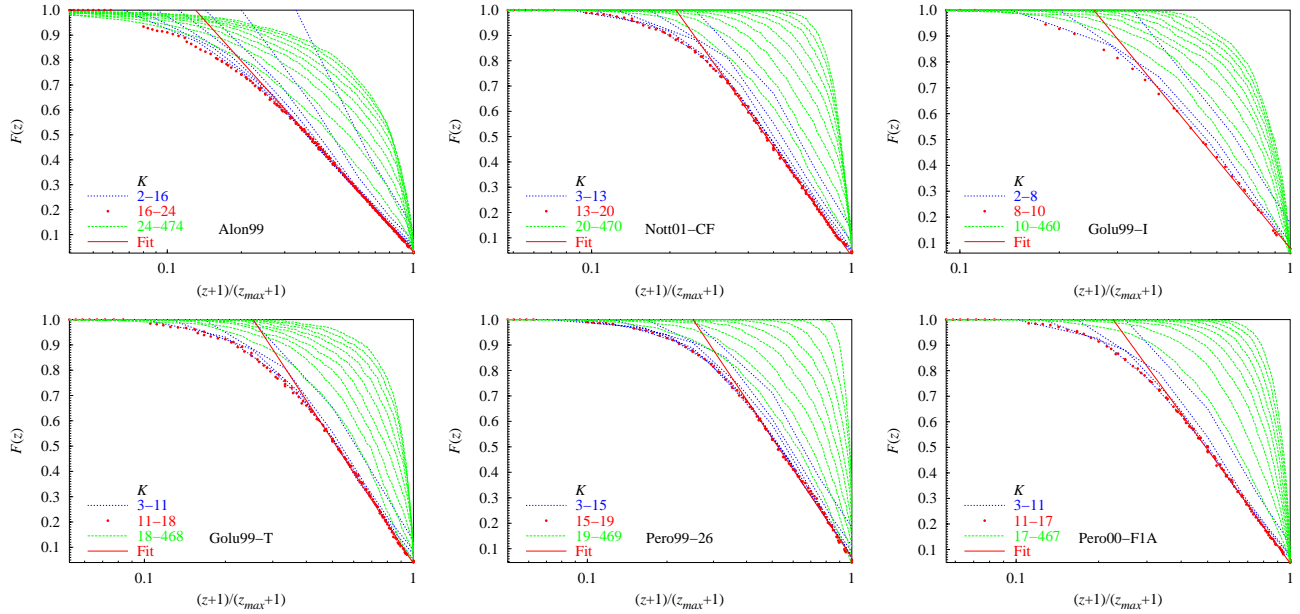


FIG. 3: Variation of cumulative probability distribution function $F(z)$ with normalized degree $(z+1)/(z_{\max}+1)$ in networks constructed from several data sets. The keys in the graphs, e.g., Alon99, correspond to the data set as described.³¹ In all the graphs, data for different types of networks (i.e., different range of K) are plotted using different line styles. Solid circles are used in the range of K corresponding to minima of $\Lambda(K)$. All these curves show a very good collapse and scale free distribution $\text{Prob}(z)$ with exponent unity in the tails. The straight solid line is least-square fit of the form given in Eq. (3) in the tails of $F(z)$. The curves drawn with dashed lines approach the solid circles as K increases (here, in steps of 2). The curves drawn with dotted lines go away from the solid circles as K increases (here, in steps of 50).

curves corresponding to the range $K_1 \leq K \leq K_2$ (solid circles) which houses the minima of the order parameter $\Lambda(K)$. The corresponding networks are highly inhomogeneous and their vertices are loosely connected. It is clear from the figure that all these curves show a very good collapse, and thus good scaling, for all the data sets. The solid straight line passing through the tails of these curves is least-square fit of the form

$$F(z) = a - b \ln \left(\frac{z+1}{z_{\max}+1} \right) \quad (3)$$

where a and b are the fit parameters. For the graphs shown in the figure, these parameters vary in the range $0.03 \leq a \leq 0.08$ and $0.47 \leq b \leq 0.71$ over all the data sets.

The extremely good fit of Eq. (3) in the tails of $F(z)$ seen in Fig. 3 implies that the corresponding probability density functions have a scale-free behavior of the form $P(z) \sim b(z+1)^{-1}$ in the tails. The power law is seen in the range $0.35 \lesssim (z+1)/(z_{\max}+1) \leq 1$ which corresponds to nearly 60% to 65% of the maximum possible range of variation of vertex degree in the network. This range is usually considered small for observing heavy tailed distributions and it is desirable to have another evidence of the scale-free character of the networks. Consequently, we analyzed the eigenvalue spectrum of the adjacency matrix of the networks.^{15,16}

Spectral density: The spectral density $\rho(\lambda)$ of the eigenvalue spectrum of the adjacency matrix of networks

$$\rho(\lambda) = \frac{1}{N} \sum_{j=1}^N \delta(\lambda - \lambda_j), \quad (4)$$

where λ_j is the j -th eigenvalue of the adjacency matrix, is a good indicator of the overall behavior of their degree distribution $P(z)$ and topological structure. For random graphs having a giant connected component $\rho(\lambda)$ is known to converge to a semicircle following the Wigner's law. Deviations from Wigner's law are seen for other cases. For small-world networks the spectral density shows a complex highly skewed structure with several blurred peaks.¹⁵ For scale free networks, the spectral density has a triangular shape with the central part lying above the semicircle.^{15,16}

Fig. 4 shows the spectral density of networks constructed from two different gene expression data sets for different values of K corresponding to the three zones of behavior of $\Lambda(K)$ seen previously. The figure shows that for small K the spectral density has an irregular shape with several blurred peaks and its bulk is confined below the semicircle. This is a characteristic of small-world networks.¹⁵ As K is increased, the bulk portion starts assuming a triangular shape which is a little skewed for small K . The top portion of the triangle starts protruding above the semicircle as K crosses K_1 . This is clear from the intermediate and high values of K in the figure. The triangular shape persists till K becomes almost equal to $N-1$. At $K = N-1$ the spectral density develops a delta function peak corresponding to $N-1$ repeated eigenvalues at $\lambda = -1$ and the largest eigenvalue is $\lambda_1 = N-1$. The above behavior of the spectral density confirms that the algorithm constructs small-world networks that become scale-free for $K \geq K_1$.

Presence of scale-free behavior indicates high degree of self-organization in the system. Such behavior is known to be

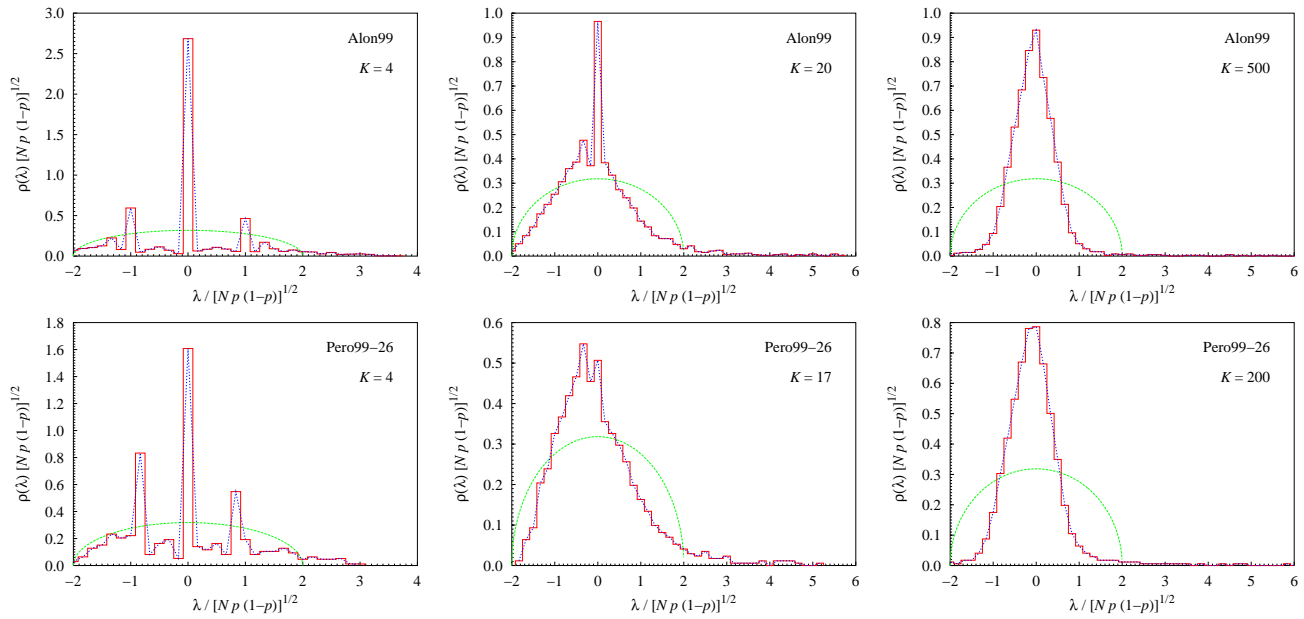


FIG. 4: Spectral density for networks constructed from two different gene expression data sets for different values of K corresponding to the three zones of behavior of the order parameter $\Lambda(K)$ (see Figs. 1 and 2). p is the fraction of edges, out of the maximum possible $N(N-1)/2$, present in the network. The semicircle corresponds to the spectral density of random networks. Dotted lines passing through middle of histograms are a guide to the eye. The keys in the graphs, e.g., Alon99, correspond to the data set as described.³¹

a characteristic of natural systems.¹⁷ It has also been observed in several natural and artificial networks, e.g., power grid,¹⁸ the Internet,^{19,20} the world-wide web,^{21,22} actor network,²³ web of human sexual contacts,²⁴ citation and collaboration networks,^{25,26} conceptual network of language,²⁷ metabolic network,²⁸ food web,²⁹ and protein networks.^{11,12} The exponents of the power-laws observed earlier, however, were always found to be more than unity. The gene networks studied here are the first examples of biological networks that show scale-free behavior with an exponent of unity. The extremely high correlations associated with this power-law have important consequences in the study of various genetic networks and associated biological processes.

The above results show that these networks are extremely inhomogeneous and contain few genes that are very highly connected and a large number of genes with low connectivity. This, in turn, implies that these networks contain large groups of co-expressed genes. As a result, the present study conclusively shows, using direct experimental data, that various types of carcinomas are a consequence of malfunction of only a few genes that either regulate the expression of a large num-

ber of other genes or form the hubs of various crowded gene regulatory pathways functioning in the organism. It is known that disturbing such genes could be fatal for the organism,³⁰ which also turns out to be the mechanism of origin of carcinomas. Identification of such genes and understanding their functionality under various conditions through which an organism can pass in its lifetime has direct relevance in the design of highly targeted drugs, among other possibilities.

The simultaneous presence of small-world and scale-free characters in these networks seems to be a perfect fit in the evolutionary scheme of biological systems. The high robustness displayed by biological systems is a consequence of the scale-free character of the associated networks. On the other hand, the fast reaction and rapid adaptability shown by biological systems can come only if the associated networks have a small-world character. This fits the structure of biological signaling system well because the chemical signaling employed at most places in biological systems, by its very nature, is very slow compared to, e.g., electrical signaling in neurons. Thus, for achieving fast message transmission, the associated networks must evolve to have small-world character.

1. Lander, E. S. Array of hope. *Nature Genet.* **21**, 3–4 (1999).
2. Gerhold, D., Rushmore, T. & Caskey, C. T. DNA chips: promising toys have become powerful tools. *Trends Biochem. Sci.* **24**, 168–173 (1999).
3. Alon, U. *et al.* Broad patterns of gene expression revealed by clustering analysis of tumor and normal colon tissues probed by oligonucleotide arrays. *Proc. Nat. Acad. Sci. USA* **96**, 6745–

6750 (1999).

4. Notterman, D. A., Alon, U., Sierk, A. J. & Levine, A. J. Transcriptional gene expression profiles of colorectal adenoma, adenocarcinoma, and normal tissue examined by oligonucleotide arrays. *Cancer Res.* **61**, 3124–3130 (2001).
5. Golub, T. R. *et al.* Molecular classification of cancer: Class discovery and class prediction by gene expression monitoring. *Sci-*

- ence **286**, 531–537 (1999).
6. Perou, C. M. *et al.* Distinctive gene expression patterns in human mammary epithelial cells and breast cancers. *Proc. Nat. Acad. Sci. USA* **96**, 9212–9217 (1999).
 7. Perou, C. M. *et al.* Molecular portraits of human breast tumors. *Nature* **406**, 747–752 (2000).
 8. Brazma, A. & Vilo, J. Gene expression data analysis. *FEBS Lett.* **480**, 17–24 (2000).
 9. Eisen, M. B., Spellman, P. T., Brown, P. O. & Botstein, D. Cluster analysis and display of genome-wide expression patterns. *Proc. Nat. Acad. Sci. USA* **95**, 14863–14868 (1998).
 10. Blatt, M., Wisemann, S. & Domany, E. Superparamagnetic clustering of data. *Phys. Rev. Lett.* **76**, 3251–3255 (1998).
 11. Jeong, H., Mason, S. P., Barabási, A.-L. & Oltvai, Z. N., Lethality and centrality in protein networks. *Nature* **411**, 41–42 (2001).
 12. Maslov, S. & Sneppen, K. Specificity and stability in topology of protein networks. *Science* **296**, 910–913 (2002).
 13. Fukunaga, K. *Introduction to statistical pattern recognition*. Academic Press, Inc. (1990).
 14. Kasteleyn, P. W. & Fortuin, C. M. Phase transitions in lattice systems with random local properties. *J. Phys. Soc. Japan, Suppl.* **26**, 11–14 (1969).
 15. Farkas, I. J., Derényi, I., Barabási, A.-L. & Vicsek, T. Spectra of “real-world” graphs: Beyond the semicircle law. *Phys. Rev. E* **64**, 026704 (2001).
 16. Goh, K.-I., Kahng, B. & Kim, D. Spectra and eigenvectors of scale-free networks. *Phys. Rev. E* **64**, 051903 (2001).
 17. Bak, P., Tang, C. & Wiesenfeld, K. Self-organized criticality: An explanation of the $1/f$ noise. *Phys. Rev. Lett.* **59**, 381–384 (1987).
 18. Watts, D. J. & Strogatz, S. H. Collective dynamics of ‘small-world’ networks. *Nature* **393**, 440–442 (1998).
 19. Cohen, R., Erez, K., ben-Avraham, D. & Havlin, S. Resilience of the Internet to random breakdowns. *Phys. Rev. Lett.* **85**, 4626–4628 (2000).
 20. Faloutsos, M., Faloutsos, P., & Faloutsos, C. On power-law relationships of Internet topology. *Compt. Commun. Rev.* **29**, 251–262 (1999).
 21. Albert, R., Jeong, H. & Barabási, A.-L. Diameter of the world-wide web. *Nature* **401**, 130–131 (1999).
 22. Huberman, B. A. & Adamic, L. A. Growth dynamics of the world-wide web. *Nature* **401**, 131 (1999).
 23. Barabási, A.-L. & Albert, R. Emergence of scaling in random networks. *Science* **286**, 509–512 (1999).
 24. Liljeros, F., Edling, C. R., Amaral, L. A. N., Stanley, H. E. & Åberg, Y. The web of human sexual contacts. *Nature* **411**, 907–908 (2001).
 25. Redner, S. How popular is your paper? An empirical study of the citation distribution. *Eur. Phys. J. B* **4**, 131–134 (1998).
 26. Newman, M. E. J. The structure of scientific collaboration networks. *Proc. Nat. Acad. Sci. USA* **98**, 404–409 (2001).
 27. Motter, A. E., de Moura, A. P. S., Lai, Y.-C. & Dasgupta, P. Topology of the conceptual network of language. *Phys. Rev. E* **65**, 065102R (2002).
 28. Jeong, H., Tombor, B., Albert, R., Oltvai, Z. N., & Barabási, A.-L. The large-scale organization of metabolic networks. *Nature* **407**, 651–654 (2000).
 29. Solé, R. V. & Montoya, J. Complexity and fragility in ecological networks. *e-print cond-mat/0011196* (2000).
 30. Hasty, J. & Collins, J. J. Unspinning the web. *Nature* **411**, 30–31 (2001).
 31. The data sets corresponding to various keys in the graphs are as follows. **Alon99**: 2000 genes in 62 samples from colon cancer data of Alon *et al.*³ **Nott01-CF**: 1211 genes in 36 samples from colon adenocarcinoma data of Notterman *et al.*⁴ We used a nominal threshold of 20 and selected genes having standard deviation at least twice the mean standard deviation in \log_2 -transformed expression data. **Golu99-I (Golu99-T)**: 1049 (1030) genes in 34 (38) samples of the independent (training) set from acute leukemia data of Golub *et al.*⁵ Genes were selected as for Nott01-CF using nominal threshold of 215 (222). **Pero99-26**: 1030 genes in 26 samples in breast cancer data of Perou *et al.*⁶ We selected genes that had good data in at least 20 samples and showed at least 2.5 fold variation above the median in at least 2 samples. **Pero00-F1A**: 1753 genes in 84 samples from breast cancer in the supplementary data of Perou *et al.*⁷

Acknowledgments: I thank Eytan Domany for introducing me to gene expression data analysis and helpful discussions, Itai Kela for help in filtering breast cancer data, and Deepak Dhar for critical review of the manuscript.

Correspondence should be addressed to H.A. (email: feagrawa@wicc.weizmann.ac.il).